Regulation of tissue oxygen levels in the mammalian lens

Richard McNulty[1,3], Huan Wang[4], Richard T. Mathias[4], Beryl J. Ortwerth[5], Roger J W. Truscott[3] and Steven Bassnett[1,2]

Departments of [1]Ophthalmology and Visual Sciences and [2]Cell Biology and Physiology, Washington University School of Medicine, St Louis, MO 63110, USA
[3]Australian Cataract Research Foundation, University of Wollongong, NSW, Australia
[4]Department of Physiology and Biophysics, SUNY, Stony Brook, NY, USA
[5]Mason Eye Institute, University of Missouri, Columbia, MO, USA

Opacification of the lens nucleus is a major cause of blindness and is thought to result from oxidation of key cellular components. Thus, long-term preservation of lens clarity may depend on the maintenance of hypoxia in the lens nucleus. We mapped the distribution of dissolved oxygen within isolated bovine lenses and also measured the rate of oxygen consumption ($\dot{Q}_{O_2}$) by lenses, or parts thereof. To assess the contribution of mitochondrial metabolism to the lens oxygen budget, we tested the effect of mitochondrial inhibitors on $\dot{Q}_{O_2}$ and partial pressure of oxygen (P_{O_2}). The distribution of mitochondria was mapped in living lenses by 2-photon microscopy. We found that a steep gradient of P_{O_2} was maintained within the tissue, leading to $P_{O_2} < 2$ mmHg in the core. Mitochondrial respiration accounted for approximately 90% of the oxygen consumed by the lens; however, P_{O_2} gradients extended beyond the boundaries of the mitochondria-containing cell layer, indicating the presence of non-mitochondrial oxygen consumers. Time constants for oxygen consumption in various regions of the lens and an effective oxygen diffusion coefficient were calculated from a diffusion–consumption model. Typical values were 3×10^{-5} cm^2 s^{-1} for the effective diffusion coefficient and a 5 min time constant for oxygen consumption. Surprisingly, the calculated time constants did not differ between differentiating fibres (DF) that contained mitochondria and mature fibres (MF) that did not. Based on these parameters, DF cells were responsible for approximately 88% of lens oxygen consumption. A modest reduction in tissue temperature resulted in a marked decrease in $\dot{Q}_{O_2}$ and the subsequent flooding of the lens core with oxygen. This phenomenon may be of clinical relevance because cold, oxygen-rich solutions are often infused into the eye during intraocular surgery. Such procedures are associated with a strikingly high incidence of postsurgical nuclear cataract.

(Resubmitted 21 May 2004; accepted after revision 14 July 2004; first published online 22 July 2004)
Corresponding author S. Bassnett: Washington University School of Medicine, Department of Ophthalmology and Visual Sciences, Campus Box 8096, 660 South Euclid Avenue, St Louis, MO 63110, USA.
Email: bassnett@vision.wustl.edu

The ocular lens consists of a mass of closely packed fibre cells bounded at the anterior by an epithelial monolayer and enveloped by a thick basement membrane, the lens capsule. Fibre cells are produced continuously by the differentiation of epithelial cells near the lens equator. Due to the steady addition of newly formed fibres, the lens grows throughout life. All cells are retained within the tissue. The oldest fibre cells are located in the centre of the lens and those that differentiated most recently are located near the surface. During terminal differentiation, all organelles (including mitochondria) are eliminated from the fibre cell cytoplasm (Bassnett, 2002). As a result, the adult lens contains two populations of fibre cells: an outer layer of differentiating fibres (DF), which contain organelles, and a core of mature fibres (MF), which do not.

Oxygen enters the lens via diffusion from the surrounding humors. Oxygen crosses cell membranes readily and, were it not consumed within the tissue, would diffuse readily into the centre of the lens. Although the lens obtains most of its energy through anaerobic glycolysis (Hockwin, 1971; van Heyningen & Linklater, 1975), a modest amount of oxidative phosphorylation occurs in the outer regions of the tissue. The consumption of oxygen in the production of ATP is expected to cause the partial pressure of oxygen (P_{O_2}) in the lens core to be lower than

 DOI: 10.1113/jphysiol.2004.068619

at the surface. In fact, Eaton (1991) and Harding (1991) have suggested that P_{O_2} throughout the lens is low, if not zero.

In vivo, the lens is situated in a relatively low oxygen environment. The average P_{O_2} in the aqueous humor of several vertebrate species is 38 mmHg (Fitch *et al.* 2000). For comparison, arterial P_{O_2} is approximately 100 mmHg. Most studies have found P_{O_2} in the vitreous humor to be significantly lower than in the aqueous humor. For example, in humans, P_{O_2} in the centre of the vitreous is approximately 16 mmHg (Sakaue *et al.* 1989; Maeda & Tano, 1996). In cat, rabbit, and chicken eyes, measurements made in the anterior vitreous, immediately adjacent to the lens, suggest P_{O_2} values of 2–3 mmHg (Jacobi & Driest, 1966; Briggs, 1973; Ormerod *et al.* 1987; Bassnett & McNulty, 2003).

The concentration and distribution of oxygen within the lens is of considerable interest clinically. In age-related nuclear cataract, cytosolic and membrane components are oxidized extensively. Protein oxidation begins in the centre of the lens and increases in severity as the cataract develops. In the most advanced cataracts, proteins in the centre of the lens are massively oxidized (Truscott & Augusteyn, 1977). The identity of the oxidant(s) responsible has not been established unequivocally. In cells of this region *de novo* protein synthesis probably does not occur (Faulkner-Jones *et al.* 2003) and, consequently, oxidized components cannot be replaced. In light of this, some authors have speculated that the effective exclusion of oxygen from the centre of the lens could be one mechanism by which cells in this region preserve their transparency over a prolonged period (Eaton, 1991). This hypothesis is supported by the interesting observation that nuclear cataracts develop in a remarkably high proportion of patients following hyperbaric oxygen (HBO) therapy (Palmquist *et al.* 1984).

Little is known about the concentration of dissolved oxygen within the normal lens. The few extant measurements of P_{O_2} (obtained using polarographic techniques) range from 1 mmHg, in the posterior cortex and nucleus of the cat (Uyama, 1973), to 21 mmHg, in the anterior cortex of the rabbit lens. In humans, P_{O_2} values of 0.8–4.0 mmHg were measured in the anterior cortex during cataract surgery (Helbig *et al.* 1993). To our knowledge, there have been no reports of the systematic mapping of P_{O_2} within any lens.

In this study, we employed a fluorescent optode technique to map P_{O_2} profiles in the isolated bovine lens. A similar approach has been employed previously to measure oxygen tension in canine ocular humors (Stefansson *et al.* 1989). We used respirometric measurements to relate the standing internal gradients of P_{O_2} to the rate of oxygen consumption ($\dot{Q}_{O_2}$). We also assessed the relative contributions of mitochondrial and non-mitochondrial oxygen consumption. Finally, we devised a quantitative model which related these parameters and provided a reasonable estimate for the effective oxygen diffusion coefficient and rate of oxygen consumption in lens cells.

Methods

Bovine lenses

Eyes were obtained from 1.5-year-old cattle after (within 6 h of) slaughter and transported on ice to the laboratory. A limbal incision was made to remove the cornea and the lens was released from the eye by carefully cutting the zonules. The average weight of dissected lenses was 2.09 ± 0.18 g (mean $\pm$ S.D.; $n = 20$). The equatorial diameter of the lenses was 16.65 ± 0.81 mm ($n = 20$) and the thickness along the polar axis was 11.05 ± 0.89 mm ($n = 20$).

Guinea pigs

Guinea pigs, which have an absolute requirement for dietary ascorbate, were used to examine the effect of ascorbate depletion on lens $\dot{Q}_{O_2}$. Adult pigmented NIH strain guinea pigs, weighing between 677 and 913 g, were randomly assigned to one of two groups. The control group was given standard guinea pig chow (Diet 5025, Purina, Richmond, IN, USA) *ad libitum*, and the experimental group was given ascorbate-free chow (Diet 5710-6 Purina) *ad libitum* for 4 weeks. Both groups were given water *ad libitum*. At the end of the 4 week period, animals were killed by CO_2 inhalation. Their lenses were removed, photographed and weighed. Lens $\dot{Q}_{O_2}$ was measured as described below. Following $\dot{Q}_{O_2}$ measurements, lenses were frozen pending HPLC determination of ascorbate content. These procedures were approved by the Washington University Animal Studies Committee.

Ascorbate analysis

Lens ascorbate was measured using an HPLC assay. Lenses were homogenized in 400 μl of 50 mM KPO_4 and 0.1 mM diethylenetriaminepentaacetic acid (DTPA). Samples were centrifuged at 19 000 ***g*** for 40 min. The supernatant was then transferred to a new tube, 100 μl of 10% metaphosphoric acid (MPA) was added, and the sample centrifuged at 19 000 ***g*** for a further 20 min. The sample was filtered by centrifuging through a 5000 nominal molecular weight limit filter. A 100 μl aliquot of the filtrate was injected into a 7.8 $\times$ 300 mm Resex RNM carbohydrate. HPLC column (Phenomenex, Torrance, CA, USA) with 1% MPA and 0.1 mM DTPA as solvent and a flow rate of 0.3 ml min^{-1} for 50 min. Suitable ascorbate standards were prepared in 0.1% MPA.

Recovery tests were performed by spiking some lens samples with known amounts of ascorbate.

Chemicals

All chemicals used were obtained from Sigma Chemical Co. (St Louis, MO, USA) unless otherwise stated.

Gasses

Custom-made gas mixtures were obtained from Airgas Inc. (St Louis, MO, USA) and contained 5% CO_2. The remainder of the gas mixture was composed of N_2.

Artificial aqueous humor solution (AAH)

Most measurements were made in artificial aqueous humor (AAH) solution. This solution resembles the aqueous humor in composition and has been used previously for physiological studies of the lens (Bassnett, 1990). The AAH had the following composition (mM): NaCl, 113; KCl, 4.5; $MgCl_2$, 1; $CaCl_2$, 1.5; D-glucose, 6; Hepes, 10; $NaHCO_3$, 20; and 1 : 1000 penicillin/streptomycin. The pH of the AAH was adjusted to pH 7.3.

Measurement of P_{O_2}

The P_{O_2} was measured using a fibre optic detection system (OxyLab, Oxford-Optronix, Oxford, UK). The oxygen sensing probe (optode) consisted of a 320 μm-wide optic fibre. An immobilized ruthenium-based fluorophore at the tip of the fibre served as the oxygen sensor. The sensor was illuminated with oscillating blue light. Fluorescence emitted by the oxygen sensor was transmitted by the fibre optic to the detector. Fluorescence lifetime was calculated automatically from the phase delay between the excitation and emission signals. The fluorescence lifetime of the fluorophore is inversely related to P_{O_2}, as described by the Stern-Volmer equation, and provides an accurate measure of P_{O_2} within the physiological range (Seddon *et al.* 2001). Optodes were obtained pre-calibrated by the manufacturer. The measurement range of the optode system was 0–100 mmHg with a resolution of 0.1 mmHg and accuracy (as reported by the manufacturer) of 0.7 mmHg. A thermocouple incorporated into the optode tip allowed temperature determination and temperature compensation of P_{O_2} measurements. Optodes measurements are reportedly insensitive to sample viscosity. To verify this, we performed preliminary measurements in a series of BSA solutions (data not shown). The P_{O_2} measurements were insensitive to protein concentration at least up to 30% (w/v) BSA (the highest value tested and the approximate protein concentration in the human lens).

After a 4 h period of equilibration in AAH at a given P_{O_2}, lenses were placed on a fenestrated stand within a custom-built Plexiglas chamber. Lenses were bathed continuously by well-mixed AAH. A gas dispersion tube in the chamber allowed AAH P_{O_2} to be regulated. The optode was mounted on a micromanipulator directly above the lens. A nick was made in the lens capsule with a 25G needle. The tip of the optode was then inserted through this small rent and advanced in millimetre increments into the lens. This usually provided 16 measurements for profiles recorded along the equatorial axis and 12 for profiles recorded along the optical axis. Only a single profile was measured in any individual lens. At each location, the optode was allowed to record a steady value (this typically took < 1 min) before being advanced once more. In this fashion, the optode was driven through the lens along either the polar or equatorial axes and corresponding P_{O_2} profiles were recorded.

Respirometry

Lens $\dot{Q}_{O_2}$ was measured using a respirometer consisting of a 5300A biological oxygen monitor, a 5301B standard bath, a 5304 microadaptor kit and a 5331A electrode (YSI Inc., Yellow Springs, OH, USA). Bovine lenses, or parts thereof, were placed in the measurement chamber in 3 ml of AAH. The P_{O_2} of the solution bathing the lens was monitored over a 20 min period and compared to a sample containing only AAH. Generally, in test samples, P_{O_2} decreased linearly over this time period, indicating that the lens was consuming oxygen from the medium. At the end of the measurement period, lenses were removed from the chamber and weighed. The $\dot{Q}_{O_2}$ (μl O_2 g^{-1} h^{-1}) was calculated from the slope of a regression line fitted to the data set. For this calculation it was assumed that 1 ml of AAH at 1 atmosphere and 37°C contained 5.02 μl of oxygen. Due to their large size, it was possible to obtain a reliable measure of $\dot{Q}_{O_2}$ on individual bovine lenses. In contrast, four guinea pig lenses were required for each $\dot{Q}_{O_2}$ determination.

Mitochondrial mapping

Although mitochondria are not present in abundance throughout the lens, they are expected to play an important role in shaping lens P_{O_2} profiles. Consequently, it was important to establish the precise distribution of mitochondria within the tissue. We took advantage of the inherent transparency of the lens to map the distribution of mitochondria in the living tissue using the vital fluorescent dye rhodamine 123 (Emaus *et al.* 1986). Fresh bovine lenses were incubated for 30 min at 37°C in AAH containing 100 μg ml^{-1} of rhodamine 123 (Molecular Probes, Eugene, OR, USA). After a brief wash, lenses were transferred to glass-bottomed Petri dishes and viewed on either a confocal (LSM 410, Carl Zeiss Inc., Thornwood, NY, USA) or 2-photon (Bio-Rad Laboratories, Hercules, CA, USA) microscope. For three dimensional reconstructions, stacks of optical sections

were collected at 4 μm intervals along the z-axis using the 2-photon microscope. The anterior polar region, the posterior polar region or the equatorial region of the lens were imaged using a 20× water immersion objective lens. Image stacks were reconstructed using volume rendering software (Autovisualize 9.1; Autoquant Imaging, Inc., Watervliet, NY, USA).

Mitochondrial distribution was also visualized by immunofluorescence using an antibody against cytochrome *c*-oxidase (A-6431, Molecular Probes). Lenses were fixed overnight in 4% paraformaldehyde–PBS. After rinsing in PBS, the lenses were boiled for 15 min in 50 mM Tris (pH 8). Lens slices (100–150 μm thick) were prepared on a tissue processor (Vibratome 1000 Plus, The Vibratome Company, St Louis, MO, USA). Samples were permeablised in 0.1% Triton X-100–PBS for 15 min, blocked with 1% BSA–10% normal goat serum–PBS for 1 h. Lens slices were incubated overnight at 4°C in 1 : 200 dilution of primary antibody in blocking solution. Slices were then washed in PBS for 30 min and incubated with goat anti-mouse IgG fluorescent secondary antibody (A-11001; Molecular Probes) at 1 : 500 in blocking solution for 2 h. Slices were mounted on slides and viewed using a confocal microscope (LSM 510, Carl Zeiss Inc., Thornwood, NY, USA).

Mitochondrial inhibition studies

The contribution of mitochondrial metabolism to lens $\dot{Q}_{O_2}$ and its role in the establishment and maintenance of intralenticular P_{O_2} gradients was examined by treatment with inhibitors of oxidative phosphorylation. Lenses were incubated in the experimental medium for 4 h prior to $\dot{Q}_{O_2}$ determination, to ensure that the internal P_{O_2} was fully equilibrated with that of the bathing medium. Mitochondrial inhibitors were added to the AAH solution during this equilibration period. We examined the effects of four different inhibitors: myxothiazol, 3-nitropropionic acid (3-NPA), sodium azide and sodium cyanide. Myxothiazol is an irreversible blocker of cytochrome b-c_1 (Thierbach & Reichenbach, 1981), 3-NPA irreversibly blocks succinate dehydrogenase (complex II) (Coles *et al.* 1979; Thierbach & Reichenbach, 1981), and sodium azide and sodium cyanide irreversibly block cytochrome *c*-oxidase (complex IV) (Leary *et al.* 1998).

Results

The bovine lens approximates an oblate spheroid with an equatorial diameter of ~17 mm and a polar diameter of ~11 mm. Because of the relatively large dimensions of the tissue, we performed a series of preliminary experiments to determine the length of time required for the internal P_{O_2} to reach a new steady state in response to a change in external P_{O_2} (Fig. 1*A*). When the external oxygen concentration was increased from 1 to 21%, a change in P_{O_2} in the centre of the lens was manifest within 30 min and complete within 4 h. Consequently, after any experimental perturbation in external P_{O_2}, lenses were incubated for at least 4 h before attempting to measure the effects on the internal P_{O_2} profile.

To determine the distribution of oxygen within the bovine lens, the optode was driven through the lens in small increments. Figure 1*B* shows an example of intralenticular P_{O_2} profiles recorded along either the polar or equatorial axis of an isolated bovine lens equilibrated with 5% external oxygen. This concentration of oxygen is similar to that surrounding the lens *in vivo* (Fitch *et al.* 2000). The main feature of traces recorded in 5% oxygen was a steep P_{O_2} gradient in the lens cortex, resulting in a uniformly low P_{O_2} in the core region. Both the polar and equatorial traces were symmetrical about the lens centre. The polar profile was not affected by the direction in which measurements were made. Thus, traces obtained by traversing the lens front-to-back were indistinguishable from those obtained back-to-front (data not shown). The cortical gradient extended 3–4 mm into the lens, although the gradient in the equatorial region often (as in the case shown in Fig. 1*B*) appeared slightly shallower than in the polar regions.

We next examined the effect on lenticular profiles of altering the P_{O_2} of the bathing medium. When incubated in solutions equilibrated with oxygen at concentrations in the physiological range (1–5%), a steep P_{O_2} gradient was recorded in the outer lens cortex (Fig. 1*C*). This was associated with a symmetrical P_{O_2} profile and extremely low P_{O_2} values in the centre of the tissue, as noted above. As the P_{O_2} in the bathing medium was increased to supra-physiological levels (21% O_2), there was a concomitant increase in lens P_{O_2}. In the centre of the lens, P_{O_2} was increased significantly and a symmetrical 'U shaped' profile resulted. This new profile was evident within a few hours of gassing the AAH with the higher oxygen concentration but did not change further on prolonged (overnight) incubation (data not shown). The profile thus represented a new steady state. Significantly, when equilibrated in solutions gassed with 21% oxygen, the standing P_{O_2} gradient was no longer confined to the outer cortex of the lens. Instead, the P_{O_2} gradient extended from the surface of the tissue to the core. When incubated in AAH equilibrated with 100% oxygen, P_{O_2} throughout the lens increased beyond the 100 mmHg upper range of the optode detection system (data not shown). The relationship between the P_{O_2} in the bathing solution and P_{O_2} in the centre of the lens is summarized in Fig. 1*D*. Note that the core P_{O_2} value did not increase significantly if the external oxygen concentration was modulated within the likely *in vivo* range. Thus, even a five-fold increase (from 1 to 5%) in external oxygen

concentration had little or no effect on P_{O_2} measured in the lens centre. In contrast, further increases in external oxygen concentration (to supraphysiological levels) were accompanied by an increase in core P_{O_2}. For example, in the presence of 21% external oxygen ($P_{O_2} \approx 150$ mmHg), lens core P_{O_2} was 30.0 ± 11.7 mmHg ($n = 7$). However, in no case did the core P_{O_2} value reach that of the bathing medium.

The mean P_{O_2} in the centre of the bovine lens was 1.6 ± 0.5 mmHg ($n = 8$) when incubated in solutions equilibrated with 5% oxygen. Because the latter approximates the concentration of oxygen surrounding the lens *in vivo*, we suspected that core P_{O_2} measured under these conditions might be close to the *in vivo* value. To obtain a better estimate of the *in vivo* core P_{O_2} value, we took the optode microsensor system to a local abattoir to record lens core P_{O_2} values as soon as possible after animals were killed. It was usually possible to complete the measurements within 15 min of death. Measurements made in this fashion indicated a core P_{O_2} value of 1.3 ± 0.5 mmHg ($n = 6$). This value did not differ significantly from that recorded *in vitro* in AAH gassed with 5% oxygen.

During fibre cell maturation, all cytoplasmic organelles are degraded (Bassnett, 2002). As a result, mitochondria are found only in newly differentiated fibre cells near the lens surface. We wished to map the spatial distribution of mitochondria within the bovine lens and relate it to intralenticular P_{O_2} gradients measured under various conditions. Using the vital fluorescent dye rhodamine 123, in conjunction with confocal and 2-photon imaging, we visualized the distribution of mitochondria in three dimensions in the living lens (Fig. 2).

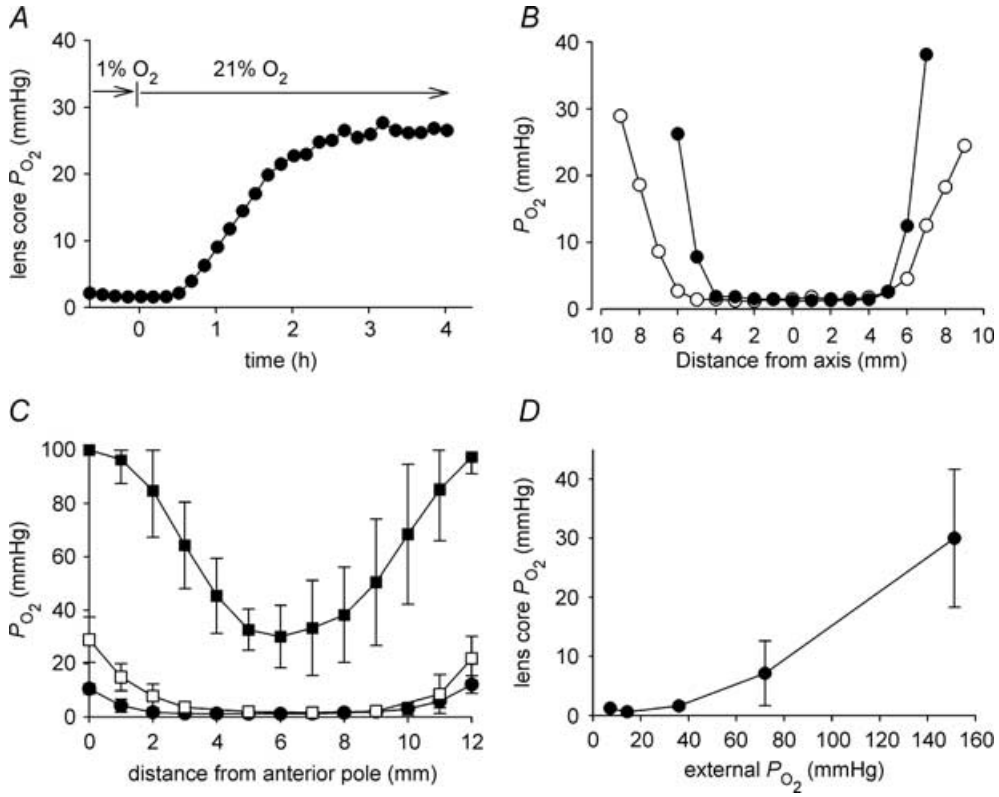

Figure 1. The relationship between internal and external P_{O_2} in the isolated bovine lens
A, the optode tip was inserted into the lens core and the response of core P_{O_2} to a change in the oxygen concentration of the bathing medium (from 1 to 21%) was monitored. Note that a new steady-state value was established within 4 h. *B*, intralenticular P_{O_2} profiles were recorded from a single lens along the polar (●) or equatorial axis (○). Measurements were made in tissue equilibrated with 5% external oxygen. The profiles are symmetric and exhibit steep cortical P_{O_2} gradients and a central region of low (1–2 mmHg) P_{O_2}. *C*, internal P_{O_2} profiles were measured in bovine lenses equilibrated with 1% (●), 5% (□), or 21% oxygen (■). In each case, data represent the mean ± S.D. of at least six independent measurements. Note that the upper measurement limit for the optode system is 100 mmHg. This value is exceeded in the peripheral cell layers of lenses incubated in 21% oxygen. The slope of the P_{O_2} profile in the outer 2–3 mm of tissue is artificially reduced as a consequence. *D*, the relationship between internal P_{O_2} (measured in the centre of the lens) and external P_{O_2} was determined in isolated bovine lenses. Note that the P_{O_2} in the centre of the lens does not increase until external P_{O_2} is raised to supraphysiological values (≥ 70 mmHg). Data represent at least six independent measurements at each oxygen concentration.

The highest concentration of mitochondria was found in the anterior epithelium (Fig. 2*A*). Consistent with previous reports on chicken and rat lenses (Bassnett & Beebe, 1992; Bantseev *et al.* 1999), we found that mitochondria in the underlying fibre cells of the bovine lens were branched, elongated structures aligned with the long axis of the fibre cells (Fig. 2*B*). Mitochondria were particularly concentrated near the fibre cell tips, in the vicinity of the anterior and posterior sutures. The cytoplasm of the anterior, equatorial, and posterior cortex was reconstructed in three dimensions (Fig. 2*C* and *D*). The depths of the mitochondria-containing layer in the anterior, equatorial and posterior cortices were 525 ± 75, 725 ± 25, and $500 \pm 25\,\mu$m, respectively ($n = 3$). To ensure that the fluorescence signal emanated specifically from lens mitochondria, some lenses were pre-treated with $100\,\mu$M carbonyl cyanide *m*-chlorophenylhydrazone (CCCP). This mitochondrial protonophore collapses the mitochondrial membrane potential (Duchen, 1999). In the presence of CCCP, fibre cell fluorescence was completely abolished (data not shown). Because rhodamine 123 is accumulated according to the mitochondrial membrane potential, the lack of fluorescence following treatment with CCCP indicated that the observed fluorescence reflected the true distribution of mitochondria within the lens. An alternative explanation for the absence of rhodamine 123 fluorescence from the lens core could be that the dye was unable to penetrate the innermost cells. To control for this, we processed some lenses for immunofluorescence and visualized the distribution of mitochondria in sagittal lens slices using an antibody against complex IV

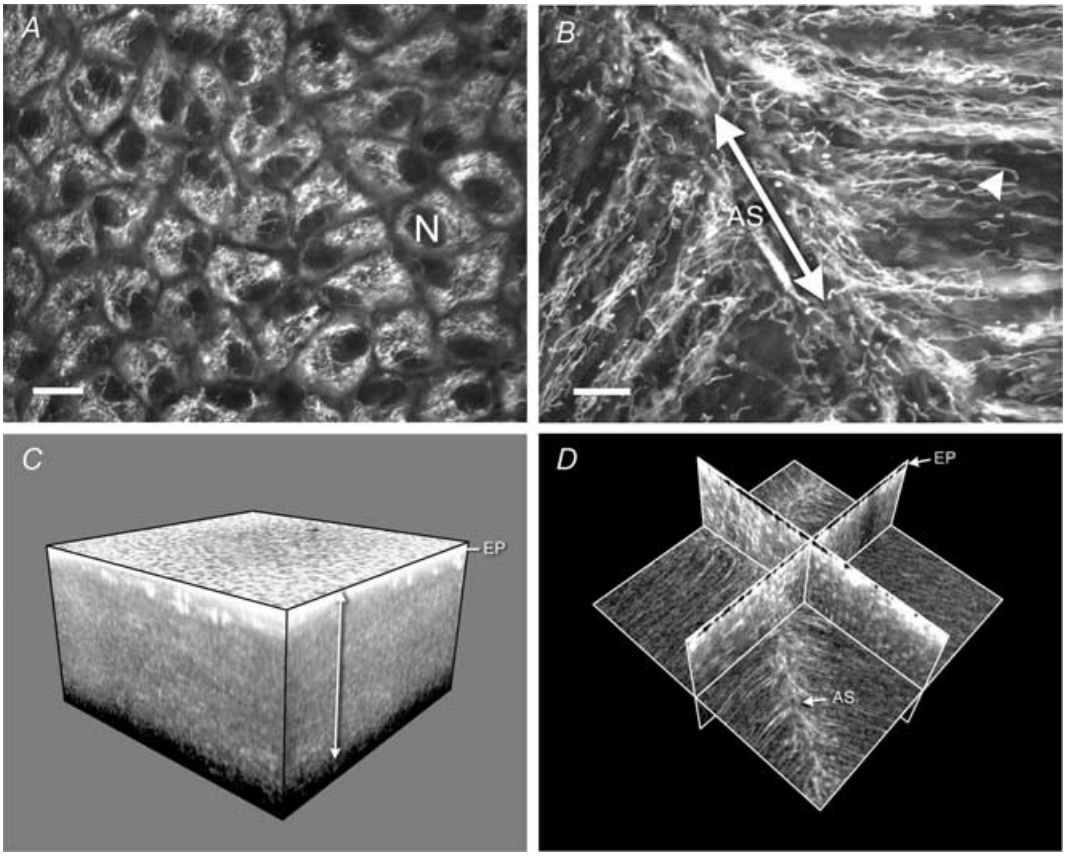

Figure 2. The distribution of mitochondria in the living bovine lens
A, a confocal image of the lens epithelium viewed *en face*. Bundles of mitochondria surround the dark, unstained epithelial cell nuclei (N). *B*, a confocal image of mitochondria located in fibre cells immediately beneath the anterior epithelium. Mitochondria were aligned with the long axis of the fibres and were particularly abundant in the region where the fibre tips converged at the anterior suture (AS). Note the elongated morphology of the mitochondria (an example of which is indicated by the arrowhead). Scale bars in *A* and $B = 10\,\mu$m. *C*, a three-dimensional reconstruction of a region ($845 \times 845 \times 476\,\mu$m) of the anterior lens cortex imaged with a 2-photon microscope. The highly fluorescent epithelium (EP) overlies a region of less intense fluorescence emanating from mitochondria located in a superficial layer of cortical fibre cells (arrowed). *D*, the same data set as *C* but viewed as a set of orthogonal planes. In this view the distribution of mitochondria within the fibres is apparent. Note the increased fluorescence adjacent to the anterior suture.

of the mitochondrial respiratory chain (data not shown). The distribution of mitochondria visualized in this fashion was qualitatively similar to that observed in the living lens using rhodamine 123 fluorescence. Measurements of the depth of mitochondria-containing cells obtained from the fixed lens slices indicated depths of $380 \pm 88\ \mu$m ($n = 3$), $305 \pm 2\ \mu$m, and $816 \pm 54\ \mu$m in the anterior, posterior and equatorial cortices, respectively. The small discrepancy between these values and those obtained from the living lens may reflect distortions that occur during processing of the fixed tissue.

The mapping studies demonstrated that the bovine lens was encircled by a continuous mitochondria-rich layer of fibre cells. At no location, however, was this layer more than 1 mm thick. The significance of this observation is that the cortical gradients measured with the optode (Fig. 1) extended approximately 4 mm beneath the tissue surface (i.e. well into the mitochondria-free core of the lens). From this we can infer that both mitochondrial and non-mitochondrial oxygen consumers are present in the lens. Driving the optode stepwise through the bovine lens sometimes caused a slight distortion in the tissue, particularly on the far side of the preparation, where the tip of the optode had to penetrate the elastic capsule to exit the lens. As a result, the total distance travelled by the optode tip sometimes slightly exceeded (by 5–10%) the actual measured diameter of the lens. We wanted to graph the data as a function of distance (r cm) from the lens centre. This required that the distance travelled by the optode be converted to the actual position (relative to the geometric centre) within the lens. We made the simplest assumption that if the total distance moved by the optode was, for example, 1.1 times the lens diameter, then each step moved the optode into the lens a factor of 0.9 times the calibrated step size. We further assumed that, at the lens surface, the P_{O_2} was the same as that in the bathing solution. With these assumptions, we were able to fit the data with a diffusion–consumption model (Appendix) that calculated P_{O_2} as a function of distance from the lens centre.

The model assumes that oxygen enters the lens by simple diffusion, with an effective diffusion coefficient D_{O_2} ($cm^2\ s^{-1}$), which depends on diffusion through membranes and cytoplasm. For oxygen, membranes are not a large diffusion barrier, so one anticipates that D_{O_2} will have a value close to that for diffusion in water. Once the oxygen enters the lens cells, it will be consumed by mitochondria or non-mitochondrial elements with time constants τ_{DF} (s) in the mitochondria-containing DF, and τ_{MF} (s) in the mitochondria-free MF. The model predicts that P_{O_2} will diminish exponentially with distance into the lens, the length constants for the exponential decrease being $\lambda_{DF} = (D_{O_2}\tau_{DF})^{0.5}$ in the DF and $\lambda_{MF} = (D_{O_2}\tau_{MF})^{0.5}$ in the MF.

The best fit of the model to empirically determined P_{O_2} profiles in 5% external oxygen is shown in Fig. 3. The curve fitting procedure provided estimates for the values of the length constants which were $\lambda_{DF} = 0.8$ mm and $\lambda_{MF} = 0.9$ mm. Given the standard deviations of the data and the assumptions intrinsic to the modelling process, these values are probably not different and we conclude that the length constants in both instances are about 1.0 mm. This conclusion was surprising, since, as previously described, the processes responsible for oxygen consumption in the DF and MF are probably different. For lenses bathed in 5% oxygen, the rate of total lens steady-state oxygen consumption was also measured at $\dot{Q}_{O_2} = 9.9\ \mu l\ h^{-1}$. This additional piece of information allowed calculation of the effective diffusion coefficient, which was $D_{O_2} = 3 \times 10^{-5}\ cm^2\ s^{-1}$, indistinguishable from that of oxygen in water (Himmelblau, 1964). This agreement with expectations provided some degree of confidence that the model is not absurdly wrong. Based on a length constant of 1 mm and a diffusion coefficient of $3 \times 10^{-5}\ cm^2\ s^{-1}$, the time constant for oxygen consumption in normal bovine lens cells is about 5 min, regardless of whether the cells are from the DF or MF zone. Again, this was a surprising conclusion and led us to address experimentally the role of mitochondria in lens oxygen consumption.

To assess the contribution of mitochondrial respiration to the oxygen budget of the bovine lens, we examined

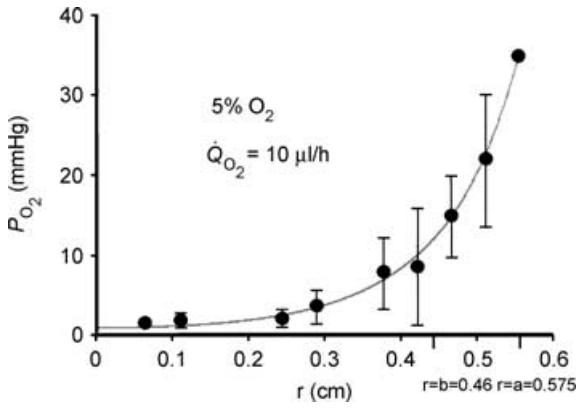

Figure 3. The best fit of the consumption–diffusion model (see Appendix) to P_{O_2} profiles measured in 5% external oxygen
The data were well fitted by the two-compartment model using Sigma Plot 2000 (SPSS Inc., Chicago, IL, USA). At 5% external oxygen, derived values for the length constants for oxygen consumption in the outer (mitochondria-rich) and central (mitochondria-free) regions of the lens were about 1 mm, which implies that the rates of oxygen consumption in these two domains are nearly the same. Based on measurements of total lens oxygen consumption ($\dot{Q}_{O_2}$) in 5% external oxygen and the best fit values of length constants, we estimate that the effective diffusion coefficient for oxygen in the lens is $3 \times 10^{-5}\ cm^2\ s^{-1}$ and the time constant for oxygen consumption within any lens cell is about 5 min. Note that 5% oxygen in the bath corresponds to a partial pressure of 36 mmHg.

the effects of four mitochondrial inhibitors on $\dot{Q}_{O_2}$ and associated internal P_{O_2} gradients. The effects of the four inhibitors were similar. Figure 4*A* shows the effect on lens $\dot{Q}_{O_2}$ of increasing concentrations of myxothiazol. In 5% oxygen, bovine lens $\dot{Q}_{O_2}$ was $4.8 \pm 0.1\ \mu l\ g^{-1}\ h^{-1}$ ($n = 10$). Myxothiazol inhibited $\dot{Q}_{O_2}$ in a dose-dependent fashion. At 1 mM, myxothiazol caused a 91% decrease in $\dot{Q}_{O_2}$, to $0.43 \pm 0.4\ \mu l\ g^{-1}\ h^{-1}$ ($n = 3$). For comparison, in 5% oxygen, 3-NPA (0.5 mM), azide (5 mM), and cyanide (10 mM) caused 66, 79 and 89.6% decreases in $\dot{Q}_{O_2}$, respectively (data not shown). Myxothiazol treatment also resulted in a concomitant change in the intralenticular P_{O_2} profile (Fig. 4*B*). In lenses equilibrated with 5% O_2, treatment with 10 μM myxothiazol caused a generalized increase in P_{O_2} at all locations within the lens. In the centre of the lens, P_{O_2} increased from 1.6 ± 0.5 ($n = 8$) to 5.3 ± 1.1 mmHg ($n = 4$). Treatment with 3-NPA (0.5 mM) or azide (5 mM) resulted in similar increases in core P_{O_2}, to 5.8 ± 0.53 ($n = 3$) and 7.7 ± 2.5 ($n = 4$), respectively.

Treatment with either myxothiazol (Fig. 4*B*) or azide (Fig. 4*C*) resulted in a change in shape of the P_{O_2} profile. In the presence of either inhibitor, P_{O_2} gradients in the outer 2 mm of the lens were markedly reduced. This led us to suspect that the inhibitors caused a significant decrease in oxygen consumption in DF cells. With zero consumption in the DF cells, the flux of oxygen through this region

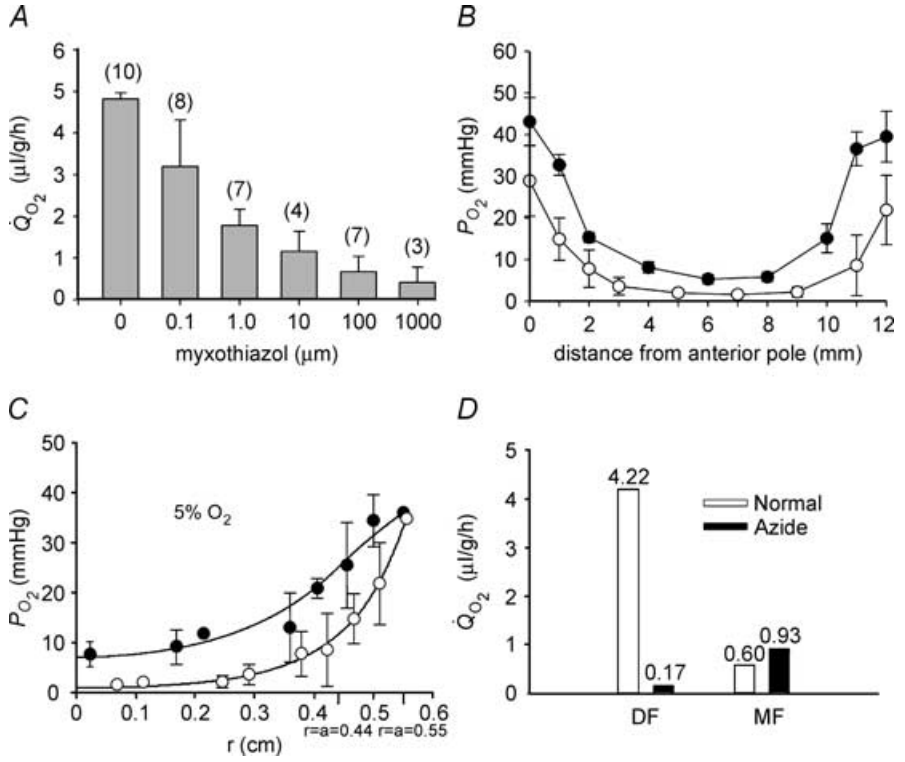

Figure 4. The effect of mitochondrial inhibitors on lens $\dot{Q}_{O_2}$, P_{O_2} profiles, and calculated oxygen consumption time constants

A, lenses were pre-equilibrated in 5% oxygen for 4 h at 37°C. Lens $\dot{Q}_{O_2}$ was inhibited by myxothiazol in a dose-dependent fashion. *B*, effect of myxothiazol on bovine lens P_{O_2} profiles *in vitro*. Lenses were equilibrated in 5% O_2 for 4 h at 37°C in the presence of 10 μM myxothiazol (●, $n = 4$). Compared to control lenses (○), myxothiazol treated lenses have a higher P_{O_2} throughout the tissue. The P_{O_2} gradient in the outer 2 mm of tissue is less steep in myxothiazol-treated lenses than controls. Note that, in each case, all data points are contained within the lens (the extreme data points nominally at 0 and 12 mm are in fact about 100 μm into the lens, explaining why the P_{O_2} values are less than the values in the superfusion solution). *C*, incubation of lenses in 5 mM azide (●) also produces a generalized increase in P_{O_2} and a shallower gradient in the superficial cell layers compared to untreated samples (○). The best fit of the diffusion–consumption model indicates that azide treatment causes a significant decrease in the rate of oxygen consumption in the outer shell of mitochondria-rich DF. *D*, the amount of oxygen consumed by the DF and MF cell layers in the presence or absence of azide was calculated using eqn (10) (Appendix). Note that, in addition to the time constants for oxygen consumption in DF and MF cells, the computed values also reflect the oxygen concentration in each region and the relative volumes of the two zones (see text for details). In the presence of azide, oxygen consumption by DF cells is dramatically reduced. In contrast, azide has little effect on oxygen consumption by the MF cells.

(J mol s^{-1}) will be constant but the flux density ($J/4\pi r^2$) will decrease towards the surface. Since the flux density is proportional to the gradient in concentration, low or no consumption in the outer shell of DF will result in a reduced slope in the concentration profile in this region.

To examine whether treatment with mitochondrial inhibitors had a differential effect on oxygen consumption in different regions of the lens, the diffusion–consumption model was fitted to the P_{O_2} profile recorded in the presence or absence of sodium azide. Under control conditions, τ_{DF} and τ_{MF} were very similar (Fig. 3). However, in the presence of azide, they differed significantly, due to a striking increase in τ_{DF} (i.e. a reduction to near zero in the rate of oxygen consumption in DF cells). The diffusion–consumption model was used to fit the azide data in Fig. 4*C* and to calculate the proportional contribution of DF and MF cells to lens oxygen consumption (Fig. 4*D*). Under control conditions, DF cells accounted for approximately 88% of the total oxygen consumed by the lens. This is due to two factors. First, because of the spherical geometry, about half the lens volume is contained in the outer shell of DF, even though this shell constitutes only the outer 20% of the radius. Second, the rate of consumption per cell is given by the concentration divided by the time constant, and the P_{O_2} in the DF is much higher than in the MF. Following treatment with azide, the calculated consumption of oxygen by the DF cell layer was drastically reduced. In contrast, azide treatment had little effect on oxygen consumption by MF cells. The modelling data thus suggested that the ~90% reduction in $\dot{Q}_{O_2}$ observed on treating lenses with mitochondrial inhibitors could be attributed to the inhibition of oxygen consumption in the outer DF layer. Nevertheless, in the presence of inhibitors, the residual oxygen consumption by MF cells was sufficient to maintain a significant gradient within the tissue, such that the core P_{O_2} remained below 10 mmHg.

The lens has a lamellar organization and, consequently, the outer fibre cells can be peeled away from the inner region. This permitted oxygen consumption in dissected regions of the bovine lens to be measured directly, using a respirometric approach. We dissected the lens into three regions: a capsule–epithelium sample, an outer cortical sample containing DF cells and an inner, core sample, containing MF cells. We measured $\dot{Q}_{O_2}$ and, in the case of the core region, P_{O_2} in these dissected lens samples (Fig. 5). The mean rate of oxygen consumption for intact lenses was $13.8 \pm 3.0\ \mu$l h^{-1} ($n = 8$) after 4 h in 21% oxygen. In contrast to the intact tissue, the dissected lens cortex was quite fragile and did not survive the 4 h equilibration period. Consequently, we were only able to measure cortical $\dot{Q}_{O_2}$ immediately after dissection. Measured in this fashion $\dot{Q}_{O_2}$ was $12.7 \pm 2.9\ \mu$l h^{-1} ($n = 7$), a value close to that obtained from the whole lens. Measurements on the lens epithelium suggested that although this layer was richly supplied with mitochondria (see Fig. 2*A*) it made only a small contribution to the overall oxygen consumption of the tissue. The epithelial $\dot{Q}_{O_2}$ was $0.4 \pm 0.4\ \mu$l h^{-1} ($n = 5$). Thus, epithelial oxygen consumption accounted for < 3% of total lens consumption.

In contrast to the cortical sample, the dense bovine lens core was a robust preparation. Consequently, we were able to measure $\dot{Q}_{O_2}$ immediately after dissection and following a 4 h equilibration period in 21% oxygen. The initial $\dot{Q}_{O_2}$ value for isolated lens cores ($5.8 \pm 1.0\ \mu$l h^{-1}) was significantly higher than the value measured after a 4 h incubation period ($1.5 \pm 0.7\ \mu$l h^{-1}). The higher initial value probably reflected passive redistribution of oxygen into the relatively hypoxic tissue, rather than oxygen consumption *per se*. A similar explanation probably accounts for the relatively high rate of consumption measured in the freshly dissected cortex. Measured at 4 h, the lens core value was approximately 11% that of the intact lens. Exposure of core samples to 10 μM myxothiazol did not cause a significant reduction in $\dot{Q}_{O_2}$ (data not shown). This provided further support for the notion that oxygen consumption in this region was not the result of mitochondrial metabolism.

We used the optode sensor to measure profiles within the dissected bovine lens cores (Fig. 5*B*, •). Although the mitochondria-containing DF cells had been removed on dissection, a significant gradient was maintained in the isolated core. Values of P_{O_2} were generally higher than in the intact lens (○) but never reached the bath value. These data support the hypothesis that the lens core contains non-mitochondrial oxygen consumers.

In some other cells, non-mitochondrial oxygen consumption can account for a significant fraction (10–20%) of total oxygen consumption (Rolfe & Brown, 1997). For example, in cells lacking mitochondrial DNA (ρ^0 cells), oxygen consumption by plasma-membrane oxido-reductases (PMOR) plays an important role, accounting for 13% of control values (Shen *et al.* 2003). In view of this finding, we treated intact lens cores or core homogenates with NADH or capsaicin, which are inhibitors of PMOR (Wolvetang *et al.* 1996). However, neither agent caused a significant decrease in core $\dot{Q}_{O_2}$ (Fig. 5*C*), suggesting that PMOR is unlikely to play a major role in oxygen consumption in the lens core. Finally, we tested whether oxygen consumption depended on the availability of free metal ions, by incubating samples with DETAPAC, a powerful chelating agent (Fisher *et al.* 2004). Although treatment of intact cores with DETAPAC had little effect, a significant reduction in $\dot{Q}_{O_2}$ was observed when core homogenates were treated. The lack of efficacy of DETAPAC on intact samples may result from poor penetration of the compound into the tissue.

Photo-oxidation is an attractive candidate for the non-mitochondrial oxygen consuming process, especially

as lenses are regularly exposed to light. Oxygen can enter an excited state (singlet oxygen or $^1O_2$) after interacting with other photolysed excited-state molecules. This highly reactive form of oxygen can engage in chemical reactions with proteins and thereby result in oxygen consumption (Davies & Truscott, 2001). However, we found that the absence of light did not significantly affect P_{O_2} profiles in the bovine lens (data not shown). Furthermore, lens $\dot{Q}_{O_2}$ in 5% O_2 was slightly higher in the dark ($5.7 \pm 1.8\ \mu l\ g^{-1}\ h^{-1}$ ($n = 4$)) than in laboratory light ($4.8 \pm 0.1\ \mu l\ g^{-1}\ h^{-1}$ ($n = 10$)). These data suggest that photo-oxidation is not an important mechanism in the control of bovine lens oxygen levels.

Ascorbate, found in unusually high concentrations in the lens, is also capable of consuming oxygen (Eaton, 1991). *In vitro* experiments demonstrated that in the

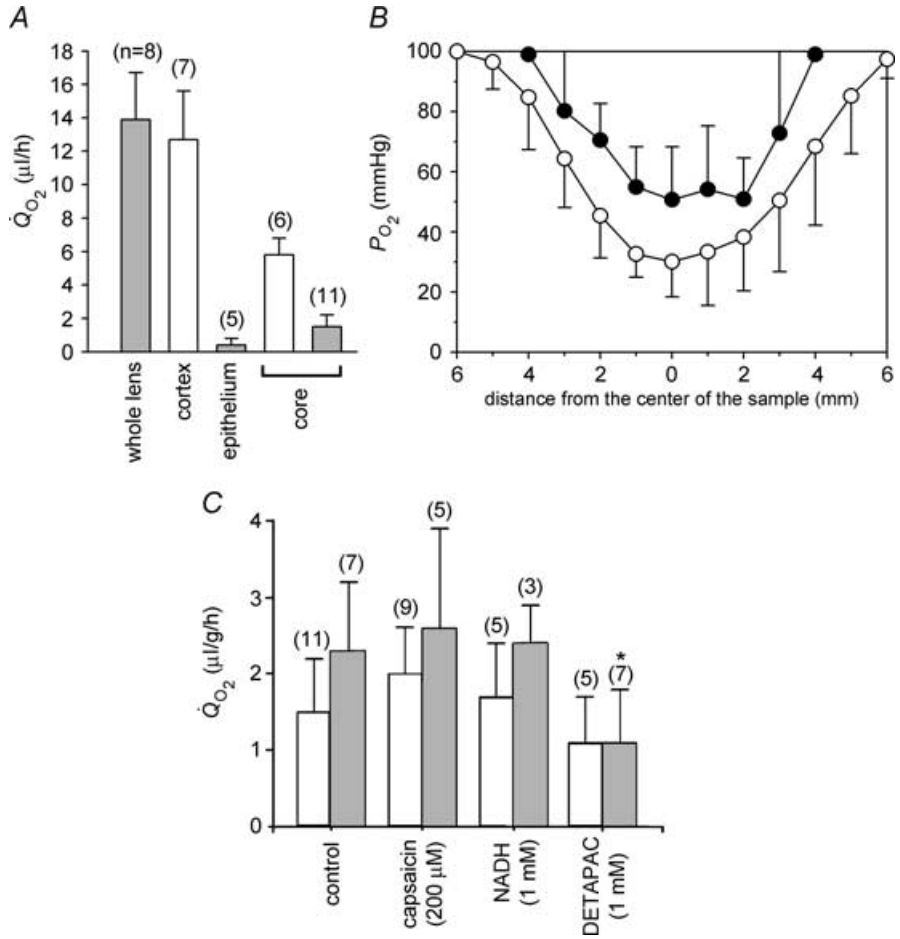

Figure 5. Measurement of $\dot{Q}_{O_2}$ and P_{O_2} profiles in regionally dissected bovine lenses
A, $\dot{Q}_{O_2}$ was measured immediately after dissection (open bars) or after a 4 h equilibration period (grey bars). Measurements were made at 37°C in solutions containing 21% oxygen. Cortical samples deteriorated over the 4 h equilibration period. Consequently, only an initial cortical measurement was possible. The relatively high $\dot{Q}_{O_2}$ value of the isolated cortex suggests that much of the oxygen consumption of the intact tissue can be attributed to the outer fibre cell layers, though some of the initial consumption represents the redistribution of oxygen from the medium into the relatively hypoxic tissue. In contrast, epithelial oxygen consumption appears to represent only a minor component (approximately 3%) of the total oxygen consumption. The $\dot{Q}_{O_2}$ values of equilibrated core samples are significantly lower than those measured immediately after dissection, again probably due to the initial redistribution of oxygen. *B*, bovine lenses were dissected to remove the DF cell layer. Isolated cores (●) were equilibrated with 21% oxygen. Data from intact lenses (taken from Fig. 1) are shown for comparison (○). Following the removal of the DF cell layer, P_{O_2} is elevated throughout the remaining core sample. However, a steep gradient persists within the core, and even after prolonged incubation, the P_{O_2} within the sample does not equal that in the bathing medium. Data represent mean ± S.D. for 5 independent measurements in each case. *C*, $\dot{Q}_{O_2}$ was measured in intact (open bars) or homogenized (grey bars) lens cores in the presence or absence of various inhibitors. The $\dot{Q}_{O_2}$ values were consistently higher in homogenized samples. Compared to control values, treatment with the PMOR inhibitors capsaicin and NADH had no significant effect on $\dot{Q}_{O_2}$ in either intact or homogenized samples. However, treatment of homogenized lens cores with the metal chelator DETAPAC resulted in a significant inhibition of $\dot{Q}_{O_2}$. Values that differ significantly ($P < 0.05$) from controls are indicated by an asterisk.

presence of trace levels of copper or iron, the oxidation of 2 mM ascorbate rapidly consumes nearly all the oxygen in the test solution (data not shown). We attempted to test the role of ascorbate directly by examining the effect of ascorbate depletion on lens $\dot{Q}_{O_2}$. For these experiments we had to use guinea pigs, which share with humans an absolute requirement for dietary ascorbate. Guinea pigs were placed on an ascorbate-free diet for 4 weeks. Lens ascorbate was then assayed by HPLC. The tissue concentration of ascorbate was calculated assuming that the water content of the guinea pig lens is similar to that reported for the rat lens (i.e. 58%) (Duncan & Jacob, 1984). Ascorbate concentrations were $696 \pm 84\,\mu$M ($n = 4$) and $88 \pm 21\,\mu$M ($n = 3$) in the control and scorbutic groups, respectively. Thus, the ascorbate-free diet led to an 87.4% reduction in lens ascorbate. Measurements on pooled guinea pig lenses indicated that $\dot{Q}_{O_2}$ was $7.0 \pm 0.8\,\mu l\,g^{-1}\,h^{-1}$ ($n = 10$ lenses) in the scorbutic group and $6.9 \pm 2.6\,\mu l\,g^{-1}\,h^{-1}$ ($n = 10$ lenses) in the control group. These values did not differ significantly. However, if ascorbate oxidation only consumes oxygen in the MF, even total depletion of ascorbate would only cause 10–20% reduction in lens oxygen consumption. Given that it was not possible to completely eliminate ascorbate from the lens, the lack of a marked inhibition of lens oxygen consumption in the scorbutic animals cannot be taken as definitive evidence against the role of ascorbate in oxygen consumption. Guinea pig lenses are small compared to the dimensions of the optode tip. Consequently, we were unable to make a parallel series of P_{O_2} measurements in the scorbutic lenses.

Due to the relatively large size of the bovine lens and the capacity of cells throughout the tissue to consume oxygen, it proved difficult to effect an increase in core P_{O_2} experimentally. Even prolonged exposure to external solutions containing supraphysiological levels of oxygen caused only a modest increase in P_{O_2} in the centre of the lens (Fig. 1). However, mitochondrial oxygen metabolism is extremely sensitive to temperature (Hulbert *et al.* 1976), and we reasoned that $\dot{Q}_{O_2}$ would be reduced by lowering the temperature and, as a consequence, that the lens core might be flooded with oxygen. Respirometric measurements of lenses bathed in 5% O_2 demonstrated that at room temperature, total lens $\dot{Q}_{O_2}$ was reduced by more than 80% compared to the values at 37°C (Fig. 6*A*). To evaluate the effect of temperature on lens P_{O_2}, the tip of the optode was positioned in the geometric centre of the lens and the temperature of the bathing medium (equilibrated with 21% oxygen) was alternated between 37°C and room temperature (~20°C). A thermocouple integrated into the tip of the optode allowed the temperature to be monitored in the lens core. A reduction in the temperature of the lens was accompanied by a rapid increase in core P_{O_2} which reversed on warming (Fig. 6*B*). Thus, oxygen homeostasis in the lens core is strongly temperature dependent.

Discussion

It has been known since 1937 that the lens consumes oxygen (Trainer cited in Ely, 1949) and does so at a rate that is only a fraction of that typically observed in other tissues. For example, oxygen uptake in the brain is $1.8\,ml\,g^{-1}\,h^{-1}$ (Van Lieshout *et al.* 2003) and in resting myocardium $3\,ml\,g^{-1}\,h^{-1}$ (Tune *et al.* 2002). These values are almost three orders of magnitude greater than those reported for lenses from a variety of species (Hans *et al.* 1955), including

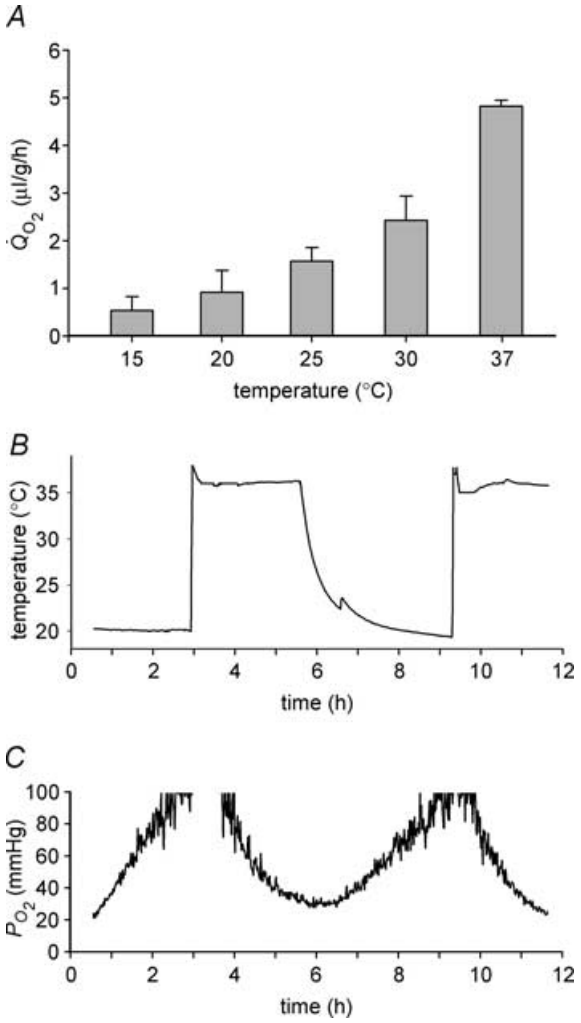

Figure 6. Effect of temperature on bovine lens $\dot{Q}_{O_2}$ and P_{O_2}
A, effect of temperature on $\dot{Q}_{O_2}$ measured in lenses equilibrated with 5% oxygen. When the temperature of the bathing medium was reduced from 37°C to room temperature (20°C) or below, $\dot{Q}_{O_2}$ fell dramatically. *B* and *C*, the P_{O_2} and temperature of the lens core were recorded as the temperature of the medium was alternated between 37°C and room temperature (~20°C). Fluctuations in the temperature of the bathing medium are paralleled (after a delay of approximately 1 h) by oscillations in core P_{O_2}.

those obtained in the current study. Nevertheless, due to the relatively large size of the lens and the absence of a blood supply, the modest rate of lens oxygen consumption results in extremely low P_{O_2} throughout much of the lens core.

Optode measurements indicated that, when perfused with solutions containing physiological levels of oxygen (= 5%), P_{O_2} in the central region of the lens was low (1.6 mmHg). From this we can calculate the tissue oxygen concentration. Values for oxygen solubility range from 1.52 μM mmHg^{-1} in serum (Groebe & Vaupel, 1988) to 1.35 μM mmHg^{-1} in pure water (Hitchman, 1978) and 0.93 μM mmHg^{-1} in tumour tissue (Grote *et al.* 1977). If we assume a comparable solubility of oxygen in the lens, then the P_{O_2} values recorded in the centre of the lens correspond to an oxygen concentration of 1–2 μM. In the current study lenses were bathed by a well stirred uniform medium. *In vivo*, however, the media bathing the anterior and posterior faces of the lens differ significantly. The aqueous humor is a relatively well-oxygenated solution that flows continuously across the anterior surface of the lens. In contrast, the vitreous humor is a gel-like structure with a very low oxygen tension. It is likely that this asymmetry will affect the shape of lens P_{O_2} profiles recorded *in vivo*. Interestingly, a recent report on the rabbit lens suggests the presence of asymmetric P_{O_2} profiles within the tissue (Barbazetto *et al.* 2004).

Our data suggest that, in the bovine lens, the majority of oxygen consumption can be attributed to the activity of mitochondria located in the outer layers of the lens. However, we consistently measured low but significant oxygen consumption in the lens core. In other tissues, scores of reactions have been identified that utilize oxygen as a substrate (Vanderkooi *et al.* 1991) and could therefore potentially contribute to oxygen consumption in the lens core. In general, the K_m for these reactions is rather high, which is consistent with the low rate of oxygen consumption measured in the present study.

We found no evidence of a role for PMOR or light in determining lens P_{O_2}. However, the role of ascorbate probably deserves further attention. In diurnal species, lens ascorbate concentration can be as high as 3 mM (Garland, 1991). In the presence of redox available metal ions, ascorbate is oxidized, forming dehydroascorbate and hydrogen peroxide and, in the process, oxygen is consumed. Dehydroascorbate is converted back to ascorbate through the oxidation of glutathione. In turn, reduced glutathione is regenerated in the surface layers of the lens via the action of glutathione reductase and NADPH (the ultimate source of the latter being hexose monophosphate shunt activity). This linked series of reactions provides a plausible pathway by which metabolic activity near the surface of the lens could facilitate non-mitochondrial oxygen consumption in the centre of the tissue. In the current study, it proved difficult to test this hypothesis directly. Treatment of core homogenates with DETAPAC resulted in a 50% reduction in oxygen consumption, indicating that at least a portion of the oxygen consumption depended on the availability of metal ions. By placing guinea pigs on an ascorbate-free diet, we were able to effect a marked (87%) reduction in the concentration of ascorbate in the lens. Such a reduction was not associated with a demonstrable decrease in lens $\dot{Q}_{O_2}$. Unfortunately these results did not allow us to rule out a role for ascorbate in non-mitochondrial oxygen consumption because, even in scorbutic animals, ascorbate was present at 88 μM, nearly two orders of magnitude greater than the concentration of dissolved oxygen in the lens core. Future experiments will therefore be required to determine the contribution, if any, of ascorbate oxidation to lens oxygen consumption.

In the presence of mitochondrial inhibitors, lens $\dot{Q}_{O_2}$ was reduced by approximately 90%. This indicates that oxidative phosphorylation is the major consumer of oxygen in the bovine lens. Interestingly, however, oxidative phosphorylation is not the major producer of ATP. In fact, numerous studies have indicated that lens ATP content is not significantly depleted following incubation in pure nitrogen or mitochondrial inhibitors (Kinoshita *et al.* 1961; Trayhurn & Van Heyningen, 1971; Winkler & Riley, 1991). Similarly, amino acid transport (Kern, 1962), sodium content (Trayhurn & Van Heyningen, 1971) and lens clarity (Giblin *et al.* 1988), are all preserved following incubation in 100% nitrogen. These data support the view that glycolysis is the major energy source for the lens and that mitochondrial respiration in the fibre cells is inconsequential with regard to many important aspects of lens homeostasis. It is believed that mitochondria and other organelles may have disappeared from the core of the mature lens in the course of evolution because they caused light scattering which reduced visual acuity. If mitochondria are not a significant source of ATP and yet by their presence degrade the optical performance of the tissue, why are they retained in the outer fibre layers? One possible explanation comes from the work of Eaton (1991). He pointed out that the best way to preserve food at room temperature in a hydrated state for a prolonged period is to can it. In the canning process, food is sealed in airtight containers from which oxygen has been removed thereby preventing oxidation and spoilage during long-term storage. This may be analogous to the situation in the lens nucleus where, in the absence of cell turnover or *de novo* protein synthesis, long-term preservation of cellular components is a prerequisite for maintaining tissue transparency. We propose therefore a novel accessory function for mitochondria in the lens: to maintain the oldest cells in the tissue (i.e. those in the lens core) in a perpetually hypoxic state. If this view is correct, it follows that conditions where mitochondrial metabolism is compromised might be associated with

an unusually high incidence of cataract. There is some support for this notion. Many inherited mitochondrial diseases are associated with an elevated risk of cataract (Ciulla *et al.* 1995; North *et al.* 1996; Finsterer *et al.* 2000), although the mechanism leading to opacification is not understood. In this regard, it is interesting to note that aged mitochondria consume significantly less oxygen than young mitochondria (Hagen *et al.* 1998). Thus, P_{O_2} could be higher in the core of aged lenses. Further experiments will be needed to test this hypothesis.

We discovered that an effective way to flood the lens core with oxygen was simply to allow the perfusate to cool to room temperature. This may be a clinically relevant observation. During vitrectomy surgery, the eye is internally perfused with cold infusion solutions equilibrated with room air (21% oxygen). Our *in vitro* experiments suggest that, under these conditions, oxygen will flood the lens core. The introduction of oxygen into the previously hypoxic tissue may have deleterious effects which could be further exacerbated by the fact that oxygen solubility is increased at lower temperatures. In the 6 months following vitrectomy surgery, 21% of patients develop cataract (Novak *et al.* 1984), and by 12 months this number rises to 63% (Van Effenterre *et al.* 1992). At 2–10 years follow up, the incidence of cataract in operated eyes ranges from 51 to 80% (Leaver *et al.* 1979; Blankenship & Machemer, 1985; Cherfan *et al.* 1991; Melberg & Thomas, 1995; Blodi & Paluska, 1997). It will be interesting to test whether by simply pre-warming the irrigating solutions the introduction of oxygen into the lens core can be prevented and, if so, whether this reduces the incidence of postvitrectomy nuclear cataract.

Appendix: lens oxygen consumption

The purpose of this appendix is to derive an approximate model of steady-state oxygen diffusion–consumption in the lens. This model can then be compared to the experimental data to obtain an estimate of the rate constants for oxygen consumption. A similar approach has been employed to model the diffusion–consumption of oxygen in the retina (Linsenmeier & Padnick-Silver, 2000).

The rate of oxygen consumption is a saturable reaction, so if C is the concentration of oxygen, then to a first approximation we can write:

$$-\frac{dC}{dt} = \frac{V_{max}C}{C+K} \quad (1)$$

where V_{max} (M s^{-1}) is the maximum rate of consumption and K (M) is the effective dissociation constant for the reaction. There are generally several paths for oxygen consumption, so eqn (1) is an effective reaction that embodies several different processes. Since eqn (1) depends non-linearly on C, it leads to differential equations that are intractable to analytic solution. However, as long as $C \ll K$, the equation is approximately linear. This assumption will clearly be valid in most regions of the lens, since the concentration of oxygen goes rapidly to near-zero as one looks from the surface into the lens. Moreover, when the concentration of oxygen in the bathing solution is not too high, this assumption will be valid everywhere. The linearized version of eqn (1) is

$$-\frac{dC}{dt} \cong C/\tau, \text{ where } \tau = K/V_{max} \quad (2)$$

The cellular structure and gross anatomy of the lens are shown in Fig. 7. The lens is somewhat spherical in shape and comprises two functionally different domains of fibre cells. For the purposes of this analysis, we will assume the lens is indeed spherical with radius a (cm). If r (cm) is the distance from the lens centre, then the outer shell of differentiating fibres (DF) is located at $b \le r \le a$ where $b \cong 0.8a$. Thus mature fibres (MF) are at $0 \le r \le b$. With regard to this analysis, the relevant difference between MF and DF is that the DF contain mitochondria, which consume oxygen, whereas the MF have no organelles (Bassnett, 2002). Thus, τ in eqn (2) takes on two values in the lens.

$$\tau = \begin{cases} \tau_{MF} \quad (s) & 0 \le r \le b \\ \tau_{DF} \quad (s) & b \le r \le a \end{cases} \quad (3)$$

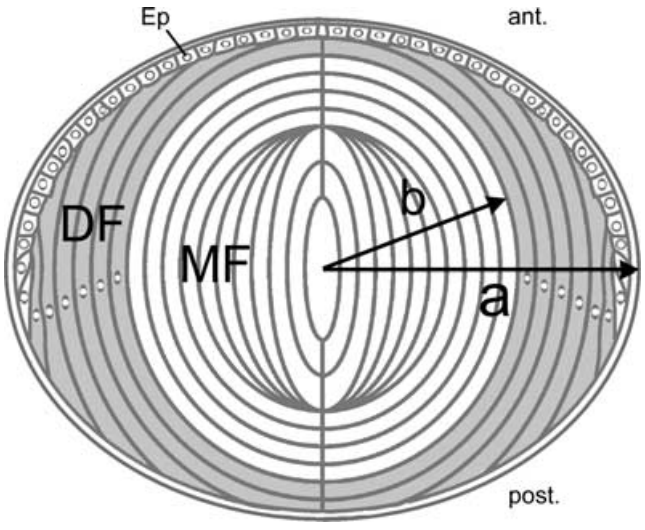

Figure 7. Diagrammatic cross-section of the lens
At the anterior (ant.), the lens is bounded by an epithelium (Ep). The bulk of the tissue is composed of concentric layers of fibre cells. Differentiating fibres (DF, shaded region) near the surface contain a normal complement of organelles. Mature fibres (MF) located in the central region of the tissue do not contain organelles. The model calculations assume a spherical lens of radius *a* (cm) in which the border between DF and MF is located at a distance *b* (cm) from the centre.

Bi-domain equations have been previously used to analyse ionic current flow in lenses from various species (reviewed in Mathias *et al.* 1997). In these equations, there are two paths for radial flow, intracellular (from cell to cell via gap junctions) and extracellular (along the narrow intercellular clefts). For ion flow, these bi-domain equations are required, since the permeability of plasma membranes for ions is very low, and hence the two paths are truly separate. However, the diffusion coefficient of oxygen in water is about 3×10^{-5} cm^2 s^{-1} (Himmelblau, 1964) whereas in plasma membrane from erythrocytes the value is about 1×10^{-5} cm^2 s^{-1} (Fischkoff & Vanderkooi, 1975), so membranes provide essentially no resistance to the diffusion of oxygen as they are very thin barriers (about 0.5% compared to cytoplasm). Hence, the concentration of oxygen in the intracellular and extracellular compartments of the lens will be essentially the same and a single effective value of D_{O_2} should be close to 3×10^{-5} cm^2 s^{-1}.

In the present study, we measure the partial pressure (P_{O_2}), which is linearly proportional to C. Thus, at this stage we will use P_{O_2} instead of C. Let P_{O_2} be our measure of the (extracellular and intracellular) concentration of oxygen. The divergence in diffusion of oxygen must equal the rate of consumption, where diffusion depends on an effective diffusion coefficient D_{O_2} (cm^2 s^{-1}) that incorporates the effects of membranes and cytoplasm. Other conditions are as follows: at the lens surface the value of $P_{O_2}(a)$ equals the concentration of oxygen in the bathing solution, defined as $P_{O_2}(\text{bath})$; at the lens centre the flux is zero; at the transition from DF to MF the concentration and flux of oxygen must be continuous. These physical requirements lead to the following differential equation and boundary conditions.

$$\begin{aligned} &D_{O_2}\frac{1}{r^2}\frac{d}{dr}\left(r^2\frac{dP_{O_2}}{dr}\right) = P_{O_2}/\tau \\ &P_{O_2}(a) = P_{O_2}(\text{bath}) \\ &\frac{dP_{O_2}(0)}{dr} = 0 \\ &P_{O_2}(b^-) = P_{O_2}(b^+) \\ &\frac{dP_{O_2}(b^-)}{dr} = \frac{dP_{O_2}(b^+)}{dr} \end{aligned} \tag{4}$$

The solutions to eqn (4) contain a common term, which we will call P1:

$$P_1 = \frac{P_{O_2}(\text{bath})}{\cosh((a-b)/\lambda_{DF})\left[\tanh((a-b)/\lambda_{DF}) + \frac{\lambda_{MF}}{\lambda_{DF}}\tanh(b/\lambda_{MF})\right]} \tag{5}$$

where

$$\begin{aligned} \lambda_{DF} &= \sqrt{D_{O_2}\tau_{DF}} \\ \lambda_{MF} &= \sqrt{D_{O_2}\tau_{MF}} \end{aligned} \tag{6}$$

The P_{O_2} profile is given by:

$$P_{O_2}(r) = P_1 \begin{cases} \frac{\lambda_{MF} a \sinh(r/\lambda_{MF})}{\lambda_{DF} r \cosh(b/\lambda_{MF})} & 0 \le r \le b \\ \frac{a \sinh((r-b)/\lambda_{DF})}{r} + \tanh(b/\lambda_{MF}) \times \frac{\lambda_{MF} a \cosh((r-b)/\lambda_{DF})}{\lambda_{DF} r} & b \le r \le a \end{cases} \tag{7}$$

At steady state there is a steep concentration gradient for oxygen in the lens, implying continuous diffusion and consumption. Total consumption (mmHg s^{-1}) within the volume of radius r must equal the rate of oxygen moving into the lens across the surface of area $4\pi r^2$:

$$\dot{Q}_{O_2}(r) = 4\pi r^2 D_{O_2}\frac{dP_{O_2}(r)}{dr} \tag{8}$$

Equation (8) can be evaluated using eqn (7) at $r = a$ to obtain total lens consumption:

$$\dot{Q}_{O_2}(a) = 4\pi a D_{O_2} P_{O_2}(\text{bath}) \times \left[\frac{a}{\lambda_{DF}}\frac{1 + \frac{\lambda_{MF}}{\lambda_{DF}}\tanh(b/\lambda_{MF})\tanh((a-b)/\lambda_{DF})}{\tanh((a-b)/\lambda_{DF}) + \frac{\lambda_{MF}}{\lambda_{DF}}\tanh(b/\lambda_{MF})} - 1\right] \tag{9}$$

Thus, we can curve-fit eqn (7) to evaluate λ_{DF} and λ_{MF}, then use eqn (9) with λ_{DF} and λ_{MF} fixed to determine D_{O_2}. Lastly, with D_{O_2}, λ_{DF} and λ_{MF} known, τ_{DF} and τ_{MF} can be determined from eqn (6). The results of this procedure are given in the text.

Once these parameters are determined, the relative oxygen consumption in the core of MF *versus* the outer shell of DF can be calculated by evaluating eqn (8) at $r = b$.

$$\dot{Q}_{O_2}(b) = 4\pi b D_{O_2} P_1 \frac{a}{\lambda_{DF}}\left(1 - \frac{\tanh(b/\lambda_{MF})}{b/\lambda_{MF}}\right) \tag{10}$$

References

Bantseev VL, Herbert KL, Trevithick JR & Sivak JG (1999). Mitochondria of rat lenses: distribution near and at the sutures. *Curr Eye Res* **19**, 506–516.

Barbazetto IA, Liang J, Chang S, Zheng L, Spector A & Dillon JP (2004). Oxygen tension in the rabbit lens and vitreous before and after vitrectomy. *Exp Eye Res* **78**, 917–924.

Bassnett S (1990). Intracellular pH regulation in the embryonic chicken lens epithelium. *J Physiol* **431**, 445–464.

Bassnett S (2002). Lens organelle degradation. *Exp Eye Res* **74**, 1–6.

Bassnett S & Beebe DC (1992). Coincident loss of mitochondria and nuclei during lens fiber cell differentiation. *Dev Dyn* **194**, 85–93.

Bassnett S & McNulty R (2003). The effect of elevated intraocular oxygen on organelle degradation in the embryonic chicken lens. *J Exp Biol* **206**, 4353–4361.

Blankenship GW & Machemer R (1985). Long-term diabetic vitrectomy results. Report of 10 year follow-up. *Ophthalmology* **92**, 503–506.

Blodi BA & Paluska SA (1997). Cataract after vitrectomy in young patients. *Ophthalmology* **104**, 1092–1095.

Briggs D & Rodenhauser JH (1973). Distribution and consumption of oxygen in the vitreous body of cats. In *Oxygen supply: theoretical and practical aspects of oxygen supply and microcirculation of tissue,* ed. Kessler M. pp. 265–269. University Park Press, Baltimore.

Cherfan GM, Michels RG, de Bustros S, Enger C & Glaser BM (1991). Nuclear sclerotic cataract after vitrectomy for idiopathic epiretinal membranes causing macular pucker. *Am J Ophthalmol* **111**, 434–438.

Ciulla TA, North K, McCabe O, Anthony DC, Korson MS & Petersen RA (1995). Bilateral infantile cataractogenesis in a patient with deficiency of complex I, a mitochondrial electron transport chain enzyme. *J Pediatr Ophthalmol Strabismus* **32**, 378–382.

Coles CJ, Edmondson DE & Singer TP (1979). Inactivation of succinate dehydrogenase by 3-nitropropionate. *J Biol Chem* **254**, 5161–5167.

Davies MJ & Truscott RJ (2001). Photo-oxidation of proteins and its role in cataractogenesis. *J Photochem Photobiol B* **63**, 114–125.

Duchen MR (1999). Contributions of mitochondria to animal physiology: from homeostatic sensor to calcium signalling and cell death. *J Physiol* **516**, 1–17.

Duncan G & Jacob TJ (1984). Influence of external calcium and glucose on internal total and ionized calcium in the rat lens. *J Physiol* **357**, 485–493.

Eaton (1991). Is the lens canned? *Free Radic Biol Med* **11**, 207–213.

Ely (1949). Metabolism of the crystalline lens. *Am J Ophthalmol* **32**, 220.

Emaus RK, Grunwald R & Lemasters JJ (1986). Rhodamine 123 as a probe of transmembrane potential in isolated rat-liver mitochondria: spectral and metabolic properties. *Biochim Biophys Acta* **850**, 436–448.

Faulkner-Jones B, Zandy AJ & Bassnett S (2003). RNA stability in terminally differentiating fibre cells of the ocular lens. *Exp Eye Res* **77**, 463–476.

Finsterer J, Bittner R, Bodingbauer M, Eichberger H, Stollberger C & Blazek G (2000). Complex mitochondriopathy associated with 4 mtDNA transitions. *Eur Neurol* **44**, 37–41.

Fischkoff S & Vanderkooi JM (1975). Oxygen diffusion in biological and artificial membranes determined by the fluorochrome pyrene. *J General Physiol* **65**, 663–676.

Fisher AE, Maxwell SC & Naughton DP (2004). Superoxide and hydrogen peroxide suppression by metal ions and their EDTA complexes. *Biochem Biophys Res Commun* **316**, 48–51.

Fitch CL, Swedberg SH & Livesey JC (2000). Measurement and manipulation of the partial pressure of oxygen in the rat anterior chamber. *Curr Eye Res* **20**, 121–126.

Garland DL (1991). Ascorbic acid and the eye. *Am J Clin Nutr* **54**, 1198S–1202S.

Giblin FJ, Schrimscher L, Chakrapani B & Reddy VN (1988). Exposure of rabbit lens to hyperbaric oxygen in vitro: regional effects on GSH level. *Invest Ophthalmol Vis Sci* **29**, 1312–1319.

Groebe K & Vaupel P (1988). Evaluation of oxygen diffusion distances in human breast cancer xenografts using tumor-specific in vivo data: role of various mechanisms in the development of tumor hypoxia. *Int J Radiat Oncol Biol Phys* **15**, 691–697.

Grote J, Susskind R & Vaupel P (1977). Oxygen diffusivity in tumor tissue (DS-carcinosarcoma) under temperature conditions within the range of 20–40 degrees C. *Pflugers Arch* **372**, 37–42.

Hagen TM, Wehr CM & Ames BN (1998). Mitochondrial decay in aging. Reversal through supplementation of acetyl-L-carnitine and N-tert-butyl-alpha-phenyl-nitrone. *Ann N Y Acad Sci* **854**, 214–223.

Hans W, Hockwin O & Kleifeld O (1955). Die bestimmung des sauerstoffverbrauches der linse auf polarographischem wege. *V Graefe's Arch Ophthal* **157**, 72–84.

Harding JJ (1991). *Cataract. Biochemistry, epidemiology and pharmacology*. Chapman and Hall. London.

Helbig H, Hinz JP, Kellner U & Foerster MH (1993). Oxygen in the anterior chamber of the human eye. *Ger J Ophthalmol* **2**, 161–164.

Himmelblau D (1964). Diffusion of dissolved gases in liquids. *Chem Rev* **64**, 527–550.

Hitchman M (1978). *Measurement of Dissolved Oxygen*. John Wiley and Sons, New York.

Hockwin O (1971). Age changes of lens metabolism. *Altern Entwickl Aging Dev* **1**, 95–129.

Hulbert AJ, Augee ML & Raison JK (1976). The influence of thyroid hormones on the structure and function of mitochondrial membranes. *Biochim Biophys Acta* **455**, 597–601.

Jacobi KW & Driest J (1966). [Oxygen determinations in the vitreous body of the living eye]. *Ber Zusammenkunft Dtsch Ophthalmol Ges* **67**, 193–198.

Kern HL (1962). Accumulation of amino acids by calf lens. *Invest Ophthalmol* **1**, 368–376.

Kinoshita JH, Kern HL & Merola LO (1961). Factors affecting the cation transport of calf lens. *Biochim Biophys Acta* **47**, 458–466.

Leary SC, Battersby BJ, Hansford RG & Moyes CD (1998). Interactions between bioenergetics and mitochondrial biogenesis. *Biochim Biophys Acta* **1365**, 522–530.

Leaver PK, Grey RH & Garner A (1979). Silicone oil injection in the treatment of massive preretinal retraction. II. Late complications in 93 eyes. *Br J Ophthalmol* **63**, 361–367.

Linsenmeier RA & Padnick-Silver L (2000). Metabolic dependence of photoreceptors on the choroid in the normal and detached retina. *Invest Ophthalmol Vis Sci* **41**, 3117–3123.

Maeda N & Tano Y (1996). Intraocular oxygen tension in eyes with proliferative diabetic retinopathy with and without vitreous. *Graefes Arch Clin Exp Ophthalmol* **234** (suppl. 1), S66–S69.

Mathias RT, Rae JL & Baldo GJ (1997). Physiological properties of the normal lens. *Physiol Rev* **77**, 21–50.

Melberg NS & Thomas MA (1995). Nuclear sclerotic cataract after vitrectomy in patients younger than 50 years of age. *Ophthalmology* **102**, 1466–1471.

North K, Korson MS, Krawiecki N, Shoffner JM & Holm IA (1996). Oxidative phosphorylation defect associated with primary adrenal insufficiency. *J Pediatr* **128**, 688–692.

Novak MA, Rice TA, Michels RG & Auer C (1984). The crystalline lens after vitrectomy for diabetic retinopathy. *Ophthalmology* **91**, 1480–1484.

Ormerod LD, Edelstein MA, Schmidt GJ, Juarez RS, Finegold SM & Smith RE (1987). The intraocular environment and experimental anaerobic bacterial endophthalmitis. *Arch Ophthalmol* **105**, 1571–1575.

Palmquist BM, Philipson B & Barr PO (1984). Nuclear cataract and myopia during hyperbaric oxygen therapy. *Br J Ophthalmol* **68**, 113–117.

Rolfe DF & Brown GC (1997). Cellular energy utilization and molecular origin of standard metabolic rate in mammals. *Physiol Rev* **77**, 731–758.

Sakaue H, Negi A & Honda Y (1989). Comparative study of vitreous oxygen tension in human and rabbit eyes. *Invest Ophthalmol Vis Sci* **30**, 1933–1937.

Seddon BM, Honess DJ, Vojnovic B, Tozer GM & Workman P (2001). Measurement of tumor oxygenation: in vivo comparison of a luminescence fiber-optic sensor and a polarographic electrode in the p22 tumor. *Radiat Res* **155**, 837–846.

Shen J, Khan N, Lewis LD, Armand R, Grinberg O, Demidenko E *et al.* (2003). Oxygen consumption rates and oxygen concentration in molt-4 cells and their mtDNA depleted (rho0) mutants. *Biophys J* **84**, 1291–1298.

Stefansson E, Peterson JI & Wang YH (1989). Intraocular oxygen tension measured with a fiber-optic sensor in normal and diabetic dogs. *Am J Physiol* **256**, H1127–H1133.

Thierbach G & Reichenbach H (1981). Myxothiazol, a new inhibitor of the cytochrome b-c1 segment of the respiratory chain. *Biochim Biophys Acta* **638**, 282–289.

Trayhurn P & Van Heyningen R (1971). Aerobic metabolism in the bovine lens. *Exp Eye Res* **12**, 315–327.

Truscott RJ & Augusteyn RC (1977). Oxidative changes in human lens proteins during senile nuclear cataract formation. *Biochim Biophys Acta* **492**, 43–52.

Tune JD, Richmond KN, Gorman MW & Feigl EO (2002). Control of coronary blood flow during exercise. *Exp Biol Med (Maywood)* **227**, 238–250.

Uyama C (1973). Diffusion model of a cat eye. In *Oxygen supply: theoretical and practical aspects of oxygen supply and microcirculation of tissue,* ed. Kessler M. pp. 64–66. University Park Press, Baltimore.

Van Effenterre G, Ameline B, Campinchi F, Quesnot S, Le Mer Y & Haut J (1992). [Is vitrectomy cataractogenic? Study of changes of the crystalline lens after surgery of retinal detachment]. *J Fr Ophtalmol* **15**, 449–454.

van Heyningen R & Linklater J (1975). The metabolism of the bovine lens in air and nitrogen. *Exp Eye Res* **20**, 393–396.

Van Lieshout JJ, Wieling W, Karemaker JM & Secher NH (2003). Syncope, cerebral perfusion, and oxygenation. *J Appl Physiol* **94**, 833–848.

Vanderkooi JM, Erecinska M & Silver IA (1991). Oxygen in mammalian tissue: methods of measurement and affinities of various reactions. *Am J Physiol* **260**, C1131–C1150.

Winkler BS & Riley MV (1991). Relative contributions of epithelial cells and fibers to rabbit lens ATP content and glycolysis. *Invest Ophthalmol Vis Sci* **32**, 2593–2598.

Wolvetang EJ, Larm JA, Moutsoulas P & Lawen A (1996). Apoptosis induced by inhibitors of the plasma membrane NADH-oxidase involves Bcl-2 and calcineurin. *Cell Growth Differ* **7**, 1315–1325.

Acknowledgements

We thank Schubert's Packing Co. (Milstadt, IL, USA), Trenton Processing Center, Inc. (Trenton, IL, USA) and Zerna Meat Co. (St Louis, MO, USA) for the bovine lenses. The authors gratefully acknowledge the expert technical assistance of Peggy Winzenburger, and Stephen Turney for his help with 2-photon microscopy. We thank Joe Bonanno and Frank Giblin for their help with preliminary experiments and Tony Hulbert for valuable discussions. This work was funded by R01 EY09852 and EY015507 (S.B.), EY02687 (Core grant for vision research), EY13570-02 (R.T.), EY06391 (R.T.M.) and an unrestricted grant to the Department of Ophthalmology and Visual Sciences from Research to Prevent Blindness (R.P.B.). S.B. is a William and Mary Greve RPB scholar.